Hindawi
Advances in Civil Engineering
Volume 2022, Article ID 9019612, 8 pages
https://doi.org/10.1155/2022/9019612

*Research Article*

# Practical Evaluation Method for the Pouring Scheme of a Long-Span Concrete-Filled Steel Tube Arch Bridge

**Xinyu Yao**,[1] **Tianzhi Hao**,[2] **and Nianchun Deng**[3]

[1]*Guangxi Transportation Science and Technology Group Co., Ltd., Nanning 530007, China*
[2]*Guangxi Beitou Traffic Maintenance Technology Group Co., Ltd., Nanning 530029, China*
[3]*College of Civil Engineering and Architecture, Guangxi University, Nanning 530004, China*

Correspondence should be addressed to Tianzhi Hao; htz0537@163.com

Received 26 April 2022; Accepted 7 June 2022; Published 21 July 2022

Academic Editor: Ilenia Farina



Concrete pouring steel tube arch is a critical part in the construction of a long-span concrete-filled steel tube arch bridge. With the adoption of the improved TOPSIS, this study summarized five indicators that controlled the concrete-filled steel tube pouring sequence. The indicators include the vertical displacement of the arch rib, lateral offset of the arch rib, steel tube stress, concrete stress, and elastic safety factor of the arch rib. Furthermore, a comprehensive objective function-rationalization index was proposed, based on which a practical evaluation and determination method for pouring scheme of the long-span concrete-filled steel tube arch bridge was developed. The results showed that a pouring sequence with relatively small stress in the arch rib, advanced alignment, and good stability could be determined using the proposed method.

## 1. Introduction

In recent 20 years, CFST arch bridge in China has developed rapidly. By 2015, more than 400 CFST arch bridges (more than 50 m) have been built in China, of which 54 have a span of more than 200 m, 11 have a span of more than 300 m, and 4 have a span of more than 400 m in China [1–5]. The completion of Hejiang No. 1 bridge marks that the concrete-filled steel tubular arch bridge has broken through the 500 m span mark. As an important construction technique for the concrete-filled steel tube arch bridge, concrete pouring in a tube is the first problem that has to be solved in order to make a remarkable improvement in the span of the concrete-filled steel tube arch bridge [6, 7]. According to the survey, many accidents were caused due to the unreasonable pouring schemes during the construction of concrete-filled steel tube arch bridges [8, 9]. In the field of determination of the optimized pouring sequence, many research works and studies were carried out. The study in [10] pointed out that different construction sequences of the arch bridge had a significant influence on the stress and stability of the structure. Therefore, the construction sequence of the arch bridge should be designed correctly in order to ensure safety during the construction process. The study in [11] considered the time-varying effect of the materials in the pouring process and suggested that the structural displacement and stress should be considered comprehensively in order to determine the pouring sequence. The study in [12] optimized the truss CFST arch bridge pouring sequence using elastic and elastic-plastic stability safety factors as indicators in order to meet the stability and safety requirements during construction. The study in [13] discussed eight representative concrete pouring sequences based on the Longbahe Super Bridge project and proposed that the evaluation of the pouring sequence should refer to the stress state of the arch foot section and the displacement state of the arch roof section. In terms of the evaluation model of the indicators, the methods proposed by scholars mainly include the comprehensive index method, analytic hierarchy process, RSR method, fuzzy comprehensive evaluation method, and gray system method [14], which is based on the life cycle assessment method [15]. Each of these methods has its characteristics, advantages, and disadvantages. Among these methods, the TOPSIS comprehensive evaluation method is

used as the decision-making method in the multiobjective decision-making analysis of limited schemes in the system. Furthermore, this method is featured a simple calculation, reasonable results, and flexible application [16–21]. There are various drawbacks to employing TOPSIS [22], and at the same time, in order to avoid the interference of human subjective factors in the process of index weighting and strengthen the objectivity of evaluation, this paper selects the entropy weight method and the improved TOPSIS model for evaluation. The entropy weight method is a method to determine the index weight by the index to be evaluated. The index weight of the scheme is mainly determined by the entropy weight method according to the influence degree of the index, and it approaches the most ideal scheme to the greatest extent according to the variation degree of each index. Also, it can effectively reflect the information implied in the data and enhance the difference and resolution of the index, so as to achieve the purpose of comprehensively reflecting all kinds of information [23, 24]. With the application of the improved TOPSIS method, this study summarized five indicators that determined the concrete-filled steel tube pouring sequence, and these include the vertical displacement and lateral offset of arch rib, steel tube transient stress, concrete transient stress, and elastic safety factor. Moreover, this study proposed a comprehensive objective function of the rationalization index and analyzed the weight matrices of the five indicators against the rationalization index based on the evaluation method and index of "optimal displacement and most favorable stress" [25]. Thus, the optimized pouring sequence was determined, which was proved theoretically and validated in practice. Furthermore, the proposed method could easily determine the optimized concrete-filled steel tube arch bridge pouring scheme, thus providing evaluation and selection reference for concrete pouring sequence optimization.

## 2. Establishment of the Practical Evaluation Method for the Pouring Scheme

The establishment of the practical evaluation method for the pouring scheme includes the mechanism of TOPSIS and the establishment procedure. They are briefly discussed.

*2.1. Mechanism of TOPSIS.* Hwang and Yoon first proposed the technique for order preference by similarity to an ideal solution (TOPSIS) in 1981 [26]. Assuming that $n$ objects need to be evaluated, then the forward matrix formed by $m$ indicators is shown in equation.

$$X = \begin{bmatrix} x_{11} & x_{12} & \cdots & x_{1m} \\ x_{21} & x_{22} & \cdots & x_{2m} \\ \vdots & \vdots & \ddots & \vdots \\ x_{n1} & x_{n2} & \cdots & x_{nm} \end{bmatrix}. \tag{1}$$

In order to eliminate the influence of dimension, the standardized matrix is denoted as **Z** and has elements as shown in equation.

$$z_{ij} = \frac{x_{ij}}{\sqrt{\sum_{i=1}^{n} x_{ij}^2}}. \tag{2}$$

After standardization, the maximum matrix is defined as $z^+ = (\max\{z_{11}, z_{21}, \cdots, z_{n1}\}, \cdots \max\{z_{1m}, z_{2m}, \cdots, z_{nm}\})$, and the minimum matrix is defined as $z^- = (\min\{z_{11}, z_{21}, \cdots, z_{n1}\}, \cdots \min\{z_{1m}, z_{2m}, \cdots, z_{nm}\})$. Then, there will be the $i$th object under evaluation $i\,(i = 1, 2, \cdots, n)$, maximum distance $D_i^+ = \sqrt{\sum_{j=1}^{m} (Z_j^+ - z_{ij})^2}$, and minimum distance $D_i^- = \sqrt{\sum_{j=1}^{m} (Z_j^- - z_{ij})^2}$. The nonnormalized score of the $i$th object is calculated $i\,(i = 1, 2, \cdots, n)$: $S_i = D_i^- / D_i^+ + D_i^-$. When $0 \le S_i \le 1$, the greater the $S_i$ value, the smaller the distance between the evaluation object and the maximum value.

*2.2. Establishment of the Practical Evaluation Method for the Pouring Scheme.* According to the five indicators of the concrete-filled steel tube pouring sequence, i.e., vertical displacement of arch ribs, lateral offset of arch ribs, steel tube transient stress, concrete transient stress, and elastic stability safety factor during the pouring process, initially, the entropy value of each index is determined. For matrix $Z = (z_{ij})_{m \times n}$, the entropy $e_j$ of parameter $j$ is given in equation.

$$e_j = -\frac{1}{\ln m} \sum_{i=1}^{m} \frac{z_{ij} + 10^{-4}}{\sum_{i=1}^{m} \left(z_{ij} + 10^{-4}\right)} \cdot \ln\left(\frac{z_{ij} + 10^{-4}}{\sum_{i=1}^{m} \left(z_{ij} + 10^{-4}\right)}\right). \tag{3}$$

Thereafter, the weight $\omega_j$ of each indicator was determined according to the variation degree as shown in equation.

$$\omega_j = \frac{\left(1 - e_j\right)}{\sum_{j=1}^{n} \left(1 - e_j\right)}. \tag{4}$$

In equation (4), $\omega_j \in [0, 1]$ and $\sum_{j=1}^{m} \omega_j = 1$.

The $i\,(i = 1, 2, \cdots, n)$th evaluation object and the maximum distance become $\tilde{D}_i^+ = \sqrt{\sum_{j=1}^{m} \omega_j (Z_j^+ - z_{ij})^2}$, and the minimum distance becomes $\tilde{D}_i^- = \sqrt{\sum_{j=1}^{m} \omega_j (Z_j^- - z_{ij})^2}$. According to the improved TOPSIS model, the objective function-rationalization index $\tilde{S}_i$ with weight and each indicator has the following form as shown in equation.

$$\tilde{S}_i = \frac{D_i^-}{D_i^+ + D_i^-}. \tag{5}$$

## 3. Practical Calculation Method

According to the above analysis, the optimized pouring scheme of the concrete-filled steel tube arch bridge is determined only by solving the rationalization index $\tilde{S}_i$ of each scheme. Due to the reasonable chemotaxis of the index system, the larger the final $\tilde{S}_i$ the more reasonable the perfusion scheme. In order to determine the optimized solution for each pouring scheme, the calculation steps are followed as follows:

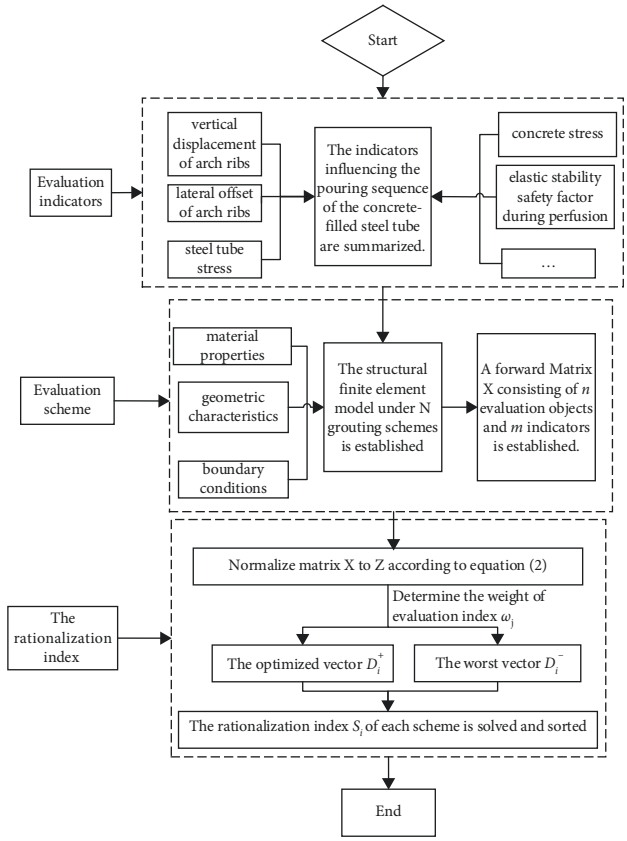


Figure 1: Flow chart of the optimized pouring scheme of the concrete-filled steel tube arch bridge.

(1) The indicators influencing the pouring sequence of the concrete-filled steel tube, such as vertical displacement of arch ribs, lateral offset of arch ribs, steel tube stress, concrete stress, and elastic stability safety factor during perfusion are summarized.

(2) The number of schemes, $n$, is determined according to the permutation and combination rule, and the finite element model is established based on different pouring sequences and different material properties, geometric characteristics, boundary conditions, and external load of the concrete-filled steel tube arch bridge. Thereafter, each index value in each scheme is calculated.

(3) Then, a forward Matrix **X** consisting of $n$ evaluation objects and $m$ indicators is established.

(4) The weight $\omega_j$ of each indicator is determined according to the variation of each indicator.

(5) Then, the forward Matrix **X** is standardized in order to eliminate the influence of different dimensions on the evaluation results, and the evaluation indexes are compared under the same dimensional system, based on the method of $z_{ij} = x_{ij}/\sqrt{\sum_{i=1}^{n} x_{ij}^2}$ to obtain Matrix **Z**.

(6) Thereafter, the optimized vector $\widetilde{D}_i^+$ and worst vector $\widetilde{D}_i^-$ are determined, in which $\widetilde{D}_i^+$ is the maximum normalization of the same evaluation indicator, and $\widetilde{D}_i^-$ is the minimum normalization of the same evaluation indicator.

(7) Finally, the rationalization index $\widetilde{S}_i$ of each scheme is solved and ranked, so that the proximity and ranking of each scheme to the ideal solution is obtained.

The flow chart for determining the optimized pouring scheme of the concrete-filled steel tube arch bridge is presented in Figure 1.

## 4. Application of the Practical Method

The application of the practical method includes that finite element modeling, calculation of the results, and analysis of the obtained results. They are discussed in the subsequent sections.

*4.1. Introduction of the Project and the Finite Element Model.* As shown in Figure 2, the main span of the concrete-filled steel tube arch bridge was taken as 575 m, and the main rib was considered to be a concrete-filled steel tube truss structure. The span was taken as 575 m, and the calculated rise-span ratio was 1/4.0. Furthermore, the arch axis coefficient was 1.50. The radial height of the vault section was taken as 8.5 m, and the radial height of the arch foot section was considered to be 17.0 m. Moreover, the rib width was taken as 4.2 m. A pair of ribs located in the upper and lower parts were installed, and these were considered to be concrete-filled steel tube strings with a diameter of 1400 mm. Thereafter, C70 concrete was considered to be poured into the tube. According to [11], there are 24 pouring sequences, which are shown in Table 1.

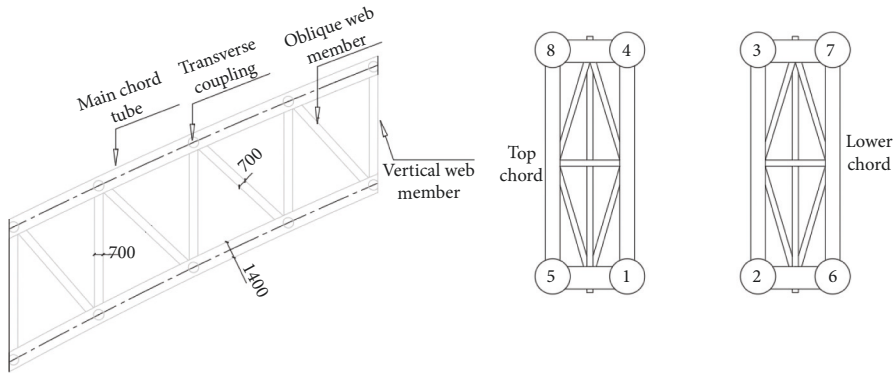


Figure 2: Cross-section of the arch rib.

Table 1: 24 pouring schemes.

| Scheme | Pouring sequence | Scheme | Pouring sequence | Scheme | Pouring sequence | Scheme | Pouring sequence |
|---|---|---|---|---|---|---|---|
| 1 | 1-2-3-4 | 7 | 2-1-4-3 | 13 | 3-4-1-2 | 19 | 4-3-2-1 |
| 2 | 1-2-4-3 | 8 | 2-1-3-4 | 14 | 3-4-2-1 | 20 | 4-3-1-2 |
| 3 | 1-3-2-4 | 9 | 2-4-1-3 | 15 | 3-1-4-2 | 21 | 4-2-3-1 |
| 4 | 1-3-4-2 | 10 | 2-4-3-1 | 16 | 3-1-2-4 | 22 | 4-2-1-3 |
| 5 | 1-4-2-3 | 11 | 2-3-1-4 | 17 | 3-2-4-1 | 23 | 4-1-3-2 |
| 6 | 1-4-3-2 | 12 | 2-3-4-1 | 18 | 3-2-1-4 | 24 | 4-1-2-3 |

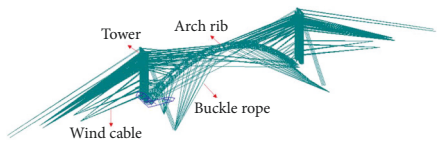


Figure 3: Finite element model of concrete pouring.

The total numbers of nodes and elements of this finite element model bridge were 12349 and 24355, respectively. The material properties, geometric characteristics, boundary conditions, and external load are the same as the data in the design drawings. The entire bridge was considered to be symmetrical. The inner tube was considered to have C70 concrete with a unit weight of 25 kN/m$^3$ and an elastic modulus of $3.7 \times 10^4$ MPa. The outer part of the arch foot section adopted C30 concrete, with a unit weight of 24 kN/m$^3$ and an elastic modulus of $3.0 \times 10^4$ MPa. The beam element was used to simulate the arch rib chord, and the double-elements method was employed to simulate the process of concrete pouring. As for the boundary conditions, the ends of the abutment and tower were fixed. Furthermore, the beam element load was applied to the corresponding position of the concrete that had not yet formed strength. After the concrete was poured, the passivation beam element load was activated by the concrete element at the same time. The finite element model is shown in Figure 3.

*4.2. Calculation Process and Results.* During analysis, 24 pouring sequence schemes were determined according to the permutation and combination rules. Based on different pouring sequences, as well as material properties, geometric characteristics, boundary conditions, and external load information of the concrete-filled steel tube arch bridge, a finite element model was established, and the corresponding index values of 24 schemes were calculated. The initial quantized value of the index is shown in Table 2.

Table 2: Initial quantization value indicator.

| Scheme | Transient stress of steel tube (MPa) | Transient stress of concrete (MPa) | Lateral offset (mm) | Maximum vertical displacement (mm) | Stability factor |
|---|---|---|---|---|---|
| 1 | −145 | 3 | 0 | -458 | 12 |
| 2 | −153 | 3 | −7 | −457 | 12 |
| 3 | −146 | 3 | −6 | −467 | 12 |
| 4 | −147 | 3 | −7 | −472 | 12 |
| 5 | −153 | 4 | −4 | −468 | 12 |
| 6 | −152 | 3 | −2 | −466 | 12 |
| 7 | −148 | 3 | −2 | −472 | 11 |
| 8 | −153 | 3 | 0 | −471 | 11 |
| 9 | −180 | 3 | −12 | −569 | 11 |
| 10 | −165 | 4 | −11 | −542 | 11 |
| 11 | −154 | 3 | −11 | −454 | 11 |
| 12 | −153 | 3 | −12 | −455 | 11 |
| 13 | −147 | 3 | −9 | −471 | 11 |
| 14 | −146 | 3 | −3 | −462 | 11 |
| 15 | −155 | 3 | −7 | −457 | 11 |
| 16 | −152 | 3 | −10 | −463 | 11 |
| 17 | −153 | 3 | −6 | −465 | 11 |
| 18 | −153 | 4 | −6 | −465 | 11 |
| 19 | −157 | 3 | −65 | −473 | 11 |
| 20 | −148 | 3 | −60 | −463 | 11 |
| 21 | −155 | 3 | −66 | −466 | 11 |
| 22 | −156 | 3 | −66 | −474 | 11 |
| 23 | −152 | 3 | −59 | −456 | 11 |
| 24 | −152 | 3 | −59 | −456 | 11 |

Finally, Matrix **X** was obtained and forwarded to obtain Matrix **Z**.

$$X = \begin{bmatrix} -145 & 1 & 0 & -458 & 12 \\ -153 & 1 & -7 & -457 & 12 \\ -146 & 1 & -6 & -467 & 12 \\ -147 & 1 & -7 & -472 & 12 \\ -153 & 0 & -4 & -468 & 12 \\ -152 & 1 & -2 & -466 & 12 \\ -148 & 1 & -2 & -472 & 11 \\ -153 & 1 & 0 & -471 & 11 \\ -180 & 1 & -12 & -569 & 11 \\ -165 & 0 & -11 & -542 & 11 \\ -154 & 1 & -11 & -454 & 11 \\ -153 & 1 & -12 & -455 & 11 \\ -147 & 1 & -9 & -471 & 11 \\ -146 & 1 & -3 & -462 & 11 \\ -155 & 1 & -7 & -457 & 11 \\ -152 & 1 & -10 & -463 & 11 \\ -153 & 1 & -6 & -465 & 11 \\ -153 & 0 & -6 & -465 & 11 \\ -157 & 1 & -65 & -473 & 11 \\ -148 & 1 & -60 & -463 & 11 \\ -155 & 1 & -66 & -466 & 11 \\ -156 & 1 & -66 & -474 & 11 \\ -152 & 1 & -59 & -456 & 11 \\ -152 & 1 & -59 & -456 & 11 \end{bmatrix},$$

$$Z = \begin{bmatrix} -0.1931 & 0.2182 & 0.0000 & -0.1979 & 0.2176 \\ -0.2037 & 0.2182 & -0.0447 & -0.1974 & 0.2176 \\ -0.1944 & 0.2182 & -0.0383 & -0.2018 & 0.2176 \\ -0.1958 & 0.2182 & -0.0447 & -0.2039 & 0.2176 \\ -0.2037 & 0.0000 & -0.0256 & -0.2022 & 0.2176 \\ -0.2024 & 0.2182 & -0.0128 & -0.2013 & 0.2176 \\ -0.1971 & 0.2182 & -0.0128 & -0.2039 & 0.1994 \\ -0.2037 & 0.2182 & 0.0000 & -0.2035 & 0.1994 \\ -0.2397 & 0.2182 & -0.0767 & -0.2458 & 0.1994 \\ -0.2197 & 0.0000 & -0.0703 & -0.2342 & 0.1994 \\ -0.2051 & 0.2182 & -0.0703 & -0.1961 & 0.1994 \\ -0.2037 & 0.2182 & -0.0767 & -0.1966 & 0.1994 \\ -0.1958 & 0.2182 & -0.0575 & -0.2035 & 0.1994 \\ -0.1944 & 0.2182 & -0.0192 & -0.1996 & 0.1994 \\ -0.2064 & 0.2182 & -0.0447 & -0.1974 & 0.1994 \\ -0.2024 & 0.2182 & -0.0639 & -0.2000 & 0.1994 \\ -0.2037 & 0.2182 & -0.0383 & -0.2009 & 0.1994 \\ -0.2037 & 0.0000 & -0.0383 & -0.2009 & 0.1994 \\ -0.2091 & 0.2182 & -0.4153 & -0.2043 & 0.1994 \\ -0.1971 & 0.2182 & -0.3833 & -0.2000 & 0.1994 \\ -0.2064 & 0.2182 & -0.4217 & -0.2013 & 0.1994 \\ -0.2077 & 0.2182 & -0.4217 & -0.2048 & 0.1994 \\ -0.2024 & 0.2182 & -0.3770 & -0.1970 & 0.1994 \\ -0.2024 & 0.2182 & -0.3770 & -0.1970 & 0.1994 \end{bmatrix}. \quad (6)$$

According to Step (6), the optimized vector $\widetilde{D}_i^+$ and the worst vector $\widetilde{D}_i^-$, as well as the rationalization index $\widetilde{S}_i$ and significance sort of each scheme, are determined as shown.

$$S_i = \begin{bmatrix} 0.0565 \\ 0.0547 \\ 0.0542 \\ 0.0539 \\ 0.0536 \\ 0.0522 \\ 0.0516 \\ 0.0514 \\ 0.0513 \\ 0.0509 \\ 0.0497 \\ 0.0489 \\ 0.0482 \\ 0.0475 \\ 0.0452 \\ 0.0366 \\ 0.0360 \\ 0.0340 \\ 0.0215 \\ 0.0215 \\ 0.0213 \\ 0.0199 \\ 0.0197 \\ 0.0197 \end{bmatrix},$$

$$\widetilde{D}_i^+ = \begin{bmatrix} 0.00 \\ 0.02 \\ 0.02 \\ 0.02 \\ 0.10 \\ 0.01 \\ 0.01 \\ 0.01 \\ 0.04 \\ 0.11 \\ 0.03 \\ 0.03 \\ 0.02 \\ 0.01 \\ 0.02 \\ 0.03 \\ 0.02 \\ 0.10 \\ 0.17 \\ 0.15 \\ 0.17 \\ 0.17 \\ 0.15 \\ 0.15 \end{bmatrix},$$

$$\widetilde{D}_i^- = \begin{bmatrix} 0.20 \\ 0.18 \\ 0.19 \\ 0.18 \\ 0.16 \\ 0.19 \\ 0.19 \\ 0.20 \\ 0.17 \\ 0.14 \\ 0.17 \\ 0.17 \\ 0.18 \\ 0.19 \\ 0.18 \\ 0.18 \\ 0.18 \\ 0.16 \\ 0.10 \\ 0.11 \\ 0.10 \\ 0.10 \\ 0.11 \\ 0.11 \end{bmatrix},$$

$$\widetilde{S}_i = \begin{bmatrix} 0.0561 \\ 0.0544 \\ 0.0536 \\ 0.0534 \\ 0.0532 \\ 0.0520 \\ 0.0513 \\ 0.0512 \\ 0.0512 \\ 0.0506 \\ 0.0495 \\ 0.0488 \\ 0.0481 \\ 0.0475 \\ 0.0447 \\ 0.0347 \\ 0.0341 \\ 0.0321 \\ 0.0232 \\ 0.0232 \\ 0.0229 \\ 0.0215 \\ 0.0214 \\ 0.0213 \end{bmatrix},$$

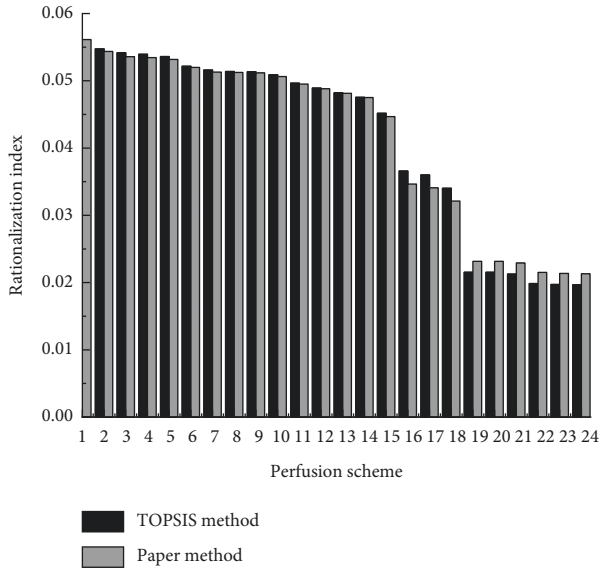


Figure 4: Rationalization indexes in different pouring schemes.

$$Sort = \begin{bmatrix} 1 \\ 6 \\ 8 \\ 7 \\ 14 \\ 3 \\ 17 \\ 4 \\ 2 \\ 15 \\ 13 \\ 16 \\ 11 \\ 12 \\ 9 \\ 5 \\ 18 \\ 10 \\ 23 \\ 24 \\ 20 \\ 19 \\ 21 \\ 22 \end{bmatrix}. \quad (7)$$

*4.3. Analysis of Calculation Results.* Furthermore, the obtained results were analyzed. The rationalization index $\widetilde{S}_i$ in each scheme was solved and then ranked, as shown in Figure 4.

Table 3: Optimal perfusion schemes obtained by different methods.

| Project | TOPSIS method | Paper method | Methods adopted in the literature [25] |
|---|---|---|---|
| Determination of the optimal scheme | Scheme 1 | Scheme 1 | Scheme 2 |
| Method characteristics | TOPSIS method has strong human subjectivity, which will affect the scheme results | It can effectively reflect the information implied in the data and enhance the difference and resolution of the index, so as to achieve the purpose of comprehensively reflecting all kinds of information. | The author only takes the minimum displacement and the minimum stress value as the only evaluation criteria |

Figure 5: Schematic diagram of on-site concrete pouring.

From Figure 4, it is observed that the improved TOPSIS model is more rational as it considers the weights of different indicators. Furthermore, among all the pouring schemes, Scheme 1 results in the maximized rationalization index (0.0561). In other words, when Scheme 1 was adopted, both the stress and deformation of the arch rib were small, indicating good stability of the structure. Then, it is also found that when the lower quarter was constructed initially and then followed by the construction of the inner part based on the rationalization indexes of these 24 schemes, it resulted in a relatively large rationalization index. Therefore, in practice, the method of "first lower quarter and then upper quarter, first inner part and then outer part" is the most effective pouring scheme. Concrete-filled steel tubular (CFST) method is a key procedure in the construction of the whole bridge. The perfusion schemes obtained by comparing various evaluation methods are shown in Table 3.

The study in [25] only takes the minimum displacement and the minimum stress value as the only evaluation criteria, and other indicators are not considered in the scheme. In addition, in order to overcome many disadvantages of the TOPSIS method, various factors should be considered. Therefore, the method in this paper is adopted, and scheme 1 is comprehensively selected for grouting. The schematic diagram of on-site concrete pouring is shown in Figure 5.

## 5. Conclusions

During the pouring process of long-span concrete-filled steel tubes, the distributions of load and stiffness on the structures are constantly changing. In addition to meeting the safety requirements during the construction stage, attention should be paid to the stability of these structures. Hence, various indicators had to be taken into consideration in the design and optimized pouring scheme. Based on the improved TOPSIS model, the evaluation and determination method of the concrete pouring sequence scheme that was proposed in this study was featured with a simple calculation, wide applicability, and fast selection of the arch rib structure with smaller stress and better linear shape. This pouring sequence with good stability and practical application could provide a reference for the construction control and optimization design of the same type of long-span concrete-filled steel tube arch bridges.

## Data Availability

All data included in this study are available from the corresponding author upon request.

## Conflicts of Interest

The authors declare that they have no conflicts of interest.

## Authors' Contributions

Conceptualization was carried out by H.T. and Y.X.; methodology was developed by H.T.; data curation was conducted by H.T.; writing of the original draft preparation was performed by Y.X and H.T.; reviewing and editing were conducted by D.C. All authors have read and agreed to the published version of the manuscript.

## Acknowledgments

This study was partly sponsored by following fund programs: 1 National Natural Science Foundation of China (Code: 51738004).2 National Natural Science Foundation of China (Code: 51868006); 3 National Natural Science Foundation of China (Code: 51878186); 4 Guangxi Natural Science Foundation cofunded cultivation project (2018GXNSFAA138067); and 5 Nanning City "Yong Jiang Project" funded project (2018-01-04).

## References

[1] B. C. Chen, "Study on the design of 600 m span concrete arch bridge," *Journal of China & Foreign Highway*, vol. 26, no. 3, pp. 21–26, 2016.

[2] J. Salonga and P. Gauvreau, "P. Comparative study of the proportions, form, and efficiency of concrete arch bridges," *Journal of Bridge Engineering*, vol. 19, no. 4, pp. 3–10, 2014.

[3] Y. Geng, Y. Ranzi, and S. Zhang, "Time-dependent behaviour of expansive concrete-filled steel tubular columns," *Journal of Constructional Steel Research*, vol. 67, no. 3, pp. 471–483, 2011.

[4] S. Li, J. Wang, and C. Yang, "Level 2 safety evaluation of concrete-filled steel tubular arch bridges incorporating structural health monitoring and inspection information based on China bridge standards," *Journal of Struct Control Health Monit*, vol. 26, no. 3, pp. 23–26, 2019.

[5] Q. Liao and J. M. Xu, "Application of prestressed intelligent tension system in construction of bridges," *Journal of Technology of Highway and Transport*, vol. 20, no. 4, pp. 102–105, 2005.

[6] Y. Geng and Y. Ding, "Out-of-plane creep buckling behavior of quadri-trussed CFST arches," *Journal of Harbin Institute of Technology*, vol. 48, no. 6, pp. 87–91, 2016.

[7] K. Xie, H. Wang, X. Guo, and J. Zhou, "Study on the safety of the concrete pouring process for the main truss arch structure in a long-span concrete-filled steel tube arch bridge," *Mechanics of Advanced Materials and Structures*, vol. 28, no. 7, pp. 731–740, 2021.

[8] B. Chen, J. Wei, and J. Zhou, "Application of concrete-filled steel tube arch bridges in China: current status and prospects," *China Civil Engineering Journal*, vol. 50, no. 6, pp. 45–50, 2017.

[9] R. Qin, X. Xie, and W. Peng, "Analysis for cracking accidents of concrete-filied-steel-tube arch bridge," *China Civil Engineering Journal*, vol. 3, pp. 74–77, 2001.

[10] N. Hao, "Construction control of 500m concrete filled steel tubular arch bridge," *Journal of Southwest Jiaotong University*, vol. 50, no. 4, pp. 635–640, 2015.

[11] Y. Zeng, A. Chen, and A. Gu, "Analysis of pouring sequence of long-span concrete filled steel tubular arch bridge considering the influence of concrete shrinkage and creep," *Journal ofProceedings of the 17th National bridge Academic Conference*, vol. 2, pp. 453–459, 2006.

[12] X. Yang, "Optimization of concrete pouring sequence of arch rib of long-span concrete-filled steel tubular arch bridge," *Journal of Highway transportation technology*, vol. 27, no. 1, pp. 67–71, 2010.

[13] M. Rosić, D. Pešić, D. Kukić, B. Antić, and M. Božović, "Method for selection of optimal road safety composite index with examples from DEA and TOPSIS method," *Accident Analysis & Prevention*, vol. 98, pp. 277–286, 2017.

[14] Y. Gui, S. Wu, and H. Ma, "Research on urban development degree based on grey correlation analysis and fuzzy comprehensive evaluation algorithm," *Journal of Computer and Digital Engineering*, vol. 50, no. 3, pp. 565–568, 2022.

[15] F. Colangelo, I. Farina, M. Travaglioni, C. Salzano, R. Cioffi, and A. Petrillo, "Eco-efficient industrial waste recycling for the manufacturing of fibre reinforced innovative geopolymer mortars: integrated waste management and green product development through LCA," *Journal of Cleaner Production*, vol. 312, Article ID 127777, 2021.

[16] J. Yang, "Tag-less sequential three branch decision model based on TOPSIS," *Journal of Shandong University*, vol. 2, pp. 1–9, 2022.

[17] B. Fan and B. Chen, "Technical condition evaluation of half-through and through arch bridges considering robustness," *Journal of Bridge Construction*, vol. 48, no. 5, pp. 64–68, 2018.

[18] Y. Yang and B. Hu, "Security evaluation of tied arch bridge based on health monitoring system," *Journal of Research and Exploration in Laboratory*, vol. 36, no. 2, pp. 5–9, 2017.

[19] Y. Yang and B. Chen, "Research on structural health monitoring system for fly-bird-type CFST arch bridge," *Journal of Highway Engineering*, vol. 40, no. 3, pp. 52–56, 2015.

[20] F. Qi and Z. Luo, "Reliability analysis of long-span CFST arch bridges based on neural network and PSO algorithm," *Journal of Shandong Agricultural University (Natural Science Edition)*, vol. 49, no. 2, pp. 331–334, 2018.

[21] J. Wang and F. Zhang, "Risk assessment of the deep-foundation pit based on the entropy weight and 2-dimensional cloud model," *Journal of Safety and Environment*, vol. 18, no. 3, pp. 849–853, 2018.

[22] Z. Shan and Y. Guo, "Evaluation of emergency logistics providers based on combined weighting- grey correlation improved TOPSIS method," *Journal of Mathematics in Practice and Theory*, vol. 49, no. 8, pp. 71–78, 2019.

[23] S. Wu and L. Huo, "Application of intuitionistic fuzzy set TOPSIS to evaluation of seismistability of slopes," *Journal of China Safety Science Journal*, vol. 27, no. 6, pp. 145–150, 2017.

[24] Y. Liao, "Evaluation method for the location selection of railway passenger station based on triangular fuzzy number," *Journal of China Railway Science*, vol. 30, no. 6, pp. 119–125, 2009.

[25] D. Pan and N. Deng, "Analysis of pouring sequence of super-long-span CFST arch bridge based on intelligent active load-control technology," *Journal of Highway*, vol. 65, no. 9, pp. 130–137, 2020.

[26] C. Hwang and K. Yoon, "Methods for multiple attribute decision making," *Multiple Attribute Decision Making*, vol. 1, pp. 58–191, 1981.